THE JOURNAL OF PHYSICAL CHEMISTRY C

pubs.acs.org/JPCC Article

Self-Assembly of a Metal–Organic Framework by Stepwise Coordination of Carboxyl and Pyrrolyl Groups

Qiang Xue, Na Xue, Jie Li, Yaru Li, Ruoning Li, Yajie Zhang, Na Li, Ziyong Shen, Shimin Hou, and Yongfeng Wang*

Cite This: J. Phys. Chem. C 2020, 124, 7790–7796

Read Online

ACCESS | Metrics & More | Article Recommendations

ABSTRACT: The coordination abilities of different functional groups play fundamental roles in metal–organic frameworks. The coordination of indole-4-carboxylic acid with Fe on surfaces was investigated by scanning tunneling microscopy and density functional theory. The carboxyl group reacted with Fe atoms to form tetramers in a deprotonation process on Au(111) at room temperature. The deprotonation of pyrrolyl groups occurred at around 350 K, forming coordinated tetramer chains and rotiform structures. The arrangement of tetrameric clusters and coordination chains on Au(100) was influenced by surface reconstitution. A two-dimensional coordination network was obtained on Ag(111) without the influence of surface reconstitution.

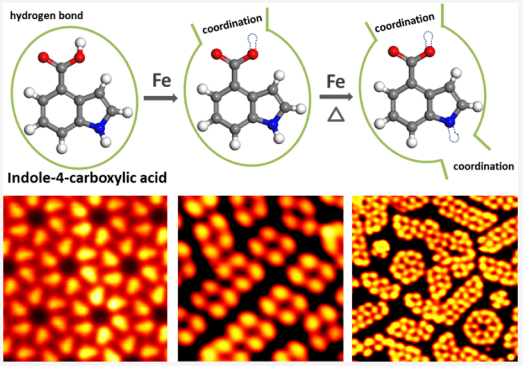

INTRODUCTION

Self-assembly of metal–organic frameworks (MOFs)[1,2] has fascinated scientists in the past decades owing to their applications in catalysis,[3] proton conductors,[4] magnetism,[5] gas storage, and separation.[6] The porous coordination architecture of MOFs provides abundant adsorption sites to capture H_2,[7] methane, acetylene,[8] and CO_2.[9] Two-dimensional (2D) MOFs on surfaces can be investigated by scanning tunneling microscopy (STM) at single-molecule level and are promising model systems for studying the structures and properties of MOFs.[10]

Various functional groups have been used to prepare surface coordination structures.[11−24] There have been reports on the coordination of carboxyl[11−13] and amidogen[14] in anionic chemical states, pyridyl,[11,15−18] bromo,[19] phenylethynyl, and cyanobiphenyl[20] groups in neutral chemical states. In most studies, the coordinated molecules only have one type of coordination group. To get more complicated structures, molecules with more than one functional group need to be investigated.

In this work, we reported a stepwise coordination of Fe and indole-4-carboxylic acid (I4CA), a bicyclic planar molecule comprising pyrrolyl and carboxyl coordination functional groups, as shown in Figure 1. We used an ultrahigh-vacuum (UHV) STM to image the topographics of Fe–I4CA coordination structures on Au(111), Au(100), and Ag(111) at 5 K. Different coordination structures of Fe–I4CA were observed, which were caused by the different coordinating abilities of the COO^- and $C_4H_4N^-$ anions. We obtained $[(Fe_2)(carboxylate)_4]$ tetrameric clusters and one-dimensional (1D) chains with $[(Fe_2)(carboxylate)_3(pyrrolyl)]$ centers on Au(111) at room temperature and 350 K, respectively. Through the templating effect of Au(100), Fe atoms and I4CA molecules yielded $[(Fe_2)(carboxylate)_4]$ tetrameric clusters oriented parallel to the reconstructed rows and 1D chains with $[(Fe_2)(carboxylate)_3(pyrrolyl)]$ centers deviated from the direction of the reconstructed rows. The coordination structures packed into two-dimensional (2D) networks on flat Ag(111) of no reconstitution. Calculations were performed using the Vienna ab initio simulation package (VASP) based on density functional theory (DFT) and pseudopotential approximation.

EXPERIMENTAL SECTION

Single-crystal Au(111), Au(100), and Ag(111) substrates were prepared through repetitive cycles of Ar ion sputtering and subsequent annealing at 673 K. The samples were characterized using an ultrahigh-vacuum (10^{-10} Torr) scanning tunneling microscope (UNISOKU, USM-1500) at a cryogenic temperature of 5 K. Fe atoms and indole-4-carboxylic acid molecules were thermally deposited from different Ta boats

Received: December 16, 2019
Revised: March 16, 2020
Published: March 18, 2020

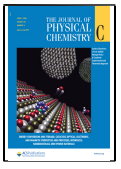

https://dx.doi.org/10.1021/acs.jpcc.9b11599
J. Phys. Chem. C 2020, 124, 7790–7796

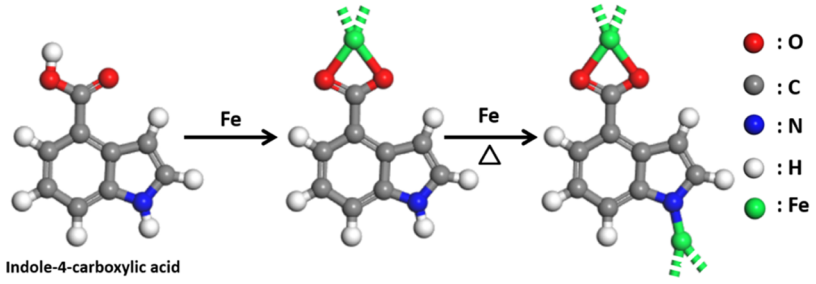

Figure 1. Two-step reaction pathway of I4CA: (1) on-surface dehydrogenation reaction of carboxylic acid with iron catalysis and (2) dehydrogenation reaction of the pyrrolyl group with iron catalysis at 350 K.

onto the metal surface held at room temperature. We annealed samples at different temperatures for 20 min to get the desired structures. All STM images (except Figure 2b) were obtained with a Pt/Ir tip under constant current mode and processed with the free software WSxM.[25]

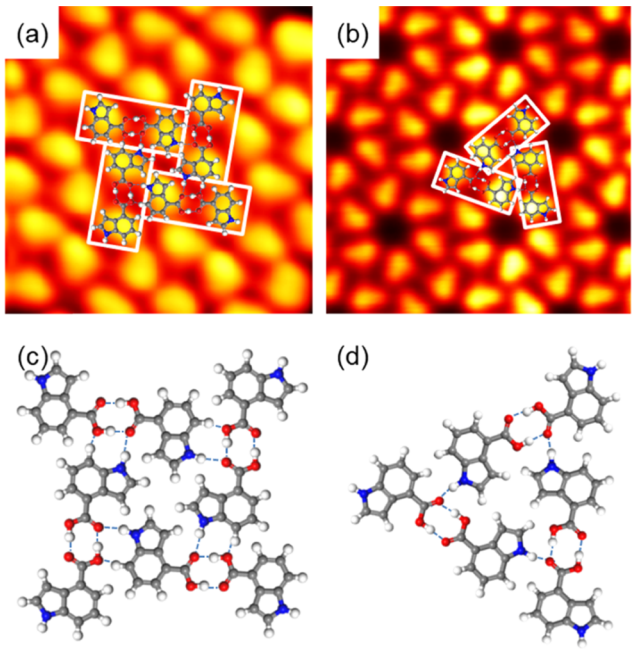

Figure 2. STM images and structural models of the indole-4-carboxylic acid (I4CA) molecules self-assembled at room temperature. Rectangular (a) and hexagonal pores (b) were formed on the Au(111) surface, as depicted in the STM images. Molecular dimers (highlighted by the white boxes in (a) and (b)) are further assembled into secondary hydrogen-bonding structures (the configurations of molecules in (a) and (b) were shown in (c) and (d)). Imaging parameters: (a) V = 100 mV, I = 50 pA, 5.0 × 5.0 nm^2; (b) constant height mode, V = 1 mV, I = 50 pA, 6.4 × 6.4 nm^2.

THEORETICAL CALCULATION

Density functional theory (DFT) calculations were performed with a Vienna ab initio simulation package (VASP) in a projector-augmented wave (PAW) framework, using a 500 eV energy cutoff for the Kohn−Sham wave functions and generalized gradient approximation (GGA) exchange−correlation energy functional. Van der Waals dispersion forces were included in the study with a γ-centered grid-sampled Brillouin zone and a vacuum of 12 Å in all directions to separate the interaction among molecules. The geometry was fully optimized when the maximum forces fell below 0.03 eV/Å.

RESULTS AND DISCUSSION

Self-assembly of I4CA molecules on Au(111) at room temperature resulted in the formation of rectangular and hexagonal porous structures (Figure 2a,b). The basic unit of both structures was a molecular dimer, constituted by H-bonding between two −COOH groups as highlighted by the white box in Figure 2a,b, which was similar to a previous study of indole-2-carboxylic acid.[26] The rectangular and hexagonal pores were composed of molecular dimers arranged in 4- or 3-fold orientations, leading to rectangular or triangular symmetric supramolecular structures, respectively. The tentative models of the two phases are shown in Figure 2c,d using DFT optimized dimers. As mentioned above, the I4CA dimer acted as the building unit of secondary rectangular and triangular supramolecular structures. After annealing the sample at 350 K, molecules were desorbed from Au(111).

The carboxylic acid reacted with Fe atoms in a dehydrogenation process to form the Fe-carboxylate metal−organic coordination structure.[12,13,27,28] Fe−I4CA coordination structures were obtained by depositing Fe atoms onto the I4CA assembly and a subsequent annealing treatment at room temperature. Figure 3a shows the representative STM image containing the tetrameric Fe−I4CA coordination structure, and Figure 3c shows the enlarged STM topograph. After comparing the image with the previous experimental results,[12,13,27,28] the carboxylate-bridged di-iron model was used to interpret the coordinated structure. The DFT optimized configuration of a tetrameric cluster is presented in Figure 3e. In the tetrameric cluster, two molecules were located at the bridging positions (antiparallel directions along the Fe−Fe axis) with the other two at the axial positions (parallel directions along the Fe−Fe axis), and the calculated Fe−Fe and the Fe−O distances were 5.1 ± 0.1 and 2.0 ± 0.1 Å, respectively. The Shockley surface state might play a role in the formation of the isolated molecular clusters shown in Figure 3.[29] Scattering of surface electrons by adsorbed molecules would lead to Friedel-type oscillations of the local density of surface states around the adsorbates, which prevents the molecular aggregation to form close-packed patterns.

After thermal annealing at 350 K, we found out that the di-iron(II) coordinated to both the carboxyl and the pyrrolyl groups. Figure 3b shows a representative STM image of the Fe−I4CA coordination chain. Similar to the other work,[30] the molecules prefer to adsorb on face-centered cubic (fcc) regions of the reconstructed surface, where the molecule−surface interaction might be stronger than that on the hexagonal close-packed (hcp) regions. Both the periodicity of the reconstruction and the relative width of fcc versus hcp domains are not changed by molecular adsorption, which indicates a rather

https://dx.doi.org/10.1021/acs.jpcc.9b11599
J. Phys. Chem. C 2020, 124, 7790−7796

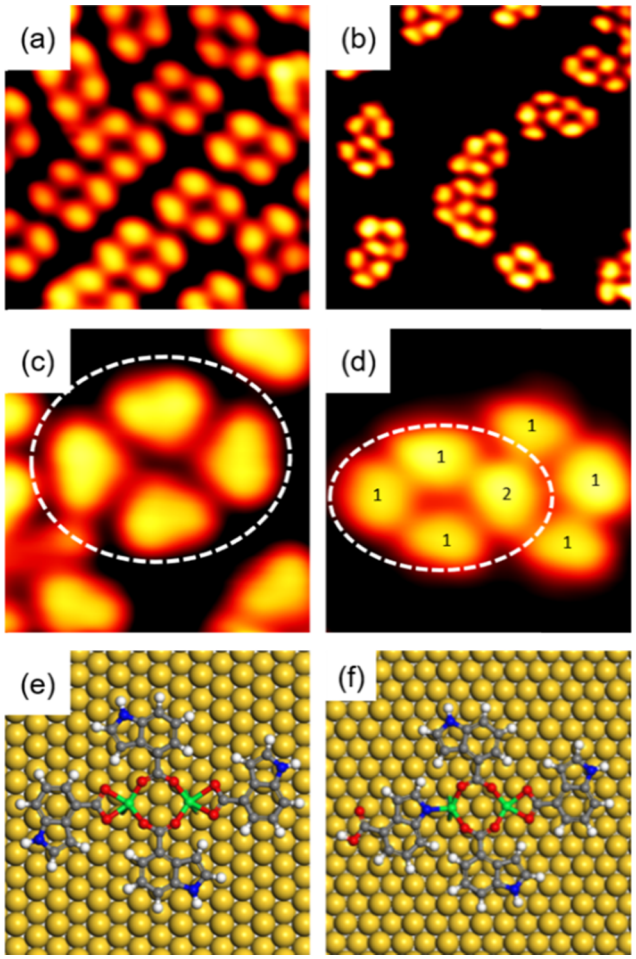

Figure 3. STM topographs of the Fe−I4CA coordination structures on Au(111): (a, c) tetrameric clusters formed at room temperature and (b, d) tetramer chains obtained at 350 K. I4CA coordinated to a Fe dimer through Fe−O and Fe−N bonds, leading to the coordination centers of $[(Fe_2)(carboxylate)_4]$ and $[(Fe_2)(carboxylate)_3(pyrrolyl)_1]$ (white circle in d) stoichiometry, respectively, and their corresponding configurations (e, f) were optimized using DFT calculation. Imaging parameters: (a) V = 1 V, I = 50 pA, 10.6 × 10.6 nm^2; (b) V = 1 V, I = 50 pA, 12.5 × 12.5 nm^2; (c) V = 10 mV, I = 50 pA, 4.0 × 4.0 nm^2; and (d) V = 1 V, I = 50 pA, 4.8 × 4.8 nm^2.

weak molecule−surface interaction. A close-up STM image (Figure 3d) shows the basic unit of the coordination chains. The inner molecules of the chain shared by two neighboring tetramers were labeled "2" and the outer molecules were labeled "1". Both the carboxyl and the pyrrolyl groups of "2" coordinated to different di-Fe(II) centers to concatenate the adjacent two tetramers. Only the carboxyl groups of "1" coordinated to individual Fe atoms. Therefore, the molecules coordinated to a Fe dimer by bridging Fe−O bonds, axial Fe−O, or Fe−N bonds, leading to the coordination centers of $[(Fe_2)(carboxylate)_x(pyrrolyl)_{4-x}]$, where x (=2, 3, 4) corresponded to the inner/outer tetramers of the coordination chains and isolated tetramers, respectively. A $[(Fe_2)(carboxylate)_3(pyrrolyl)_1]$ motif containing carboxyl groups at the bridging positions and pyrrolyl groups at the axial positions, as highlighted by the white circle in Figure 3d, was optimized by DFT calculations and is depicted in Figure 3f. The optimized Fe−O and Fe−N distances were 2.0 and 1.9 Å, respectively.

When annealing the sample at 400 K, the predominant structures were coordination tetramer chains and a few new wheel-like supramolecular motifs were also observed on the surface, as shown in Figure 4a. The ratio of the number of 14CA molecules in the chains versus that in the rotiform structures amounted to 84:16. The width and length of the tetramer chain (Figure 4b) were confined by the Au herringbones, as was the orientation, which was strictly determined by the local orientation of the Au(111) herringbone reconstruction. The molecular model is displayed in Figure 4e. Five or six Fe-coordinated tetramers with shared molecules were encircled into loops forming rotiform structures (Figure 4c,d). The corresponding molecular models of the rotiform structures of five or six hubs are shown in Figure 4f,g. I4CA molecules acted as "joint" molecules concatenating two adjacent tetramers in these three different supramolecules. The absorption chirality of the joint molecules marked in red and blue in Figure 4e−g determined the extending direction of the coordination structures. If the absorption chiralities of the joint molecules of two adjacent tetramers differed, linear structures were formed. In the case of homo-chiral joint molecules, rotiform structures were constructed instead. The angle between the long axes of two adjacent tetramers caused by steric hindrance was another influencing factor, with the most stable angle being 65°. The angles of 72 and 60° appeared owing to specific steric arrangements to resist the distortion of bonds.

The arrangement of the coordinated tetramer chains (Figure 4b) was confined by the Au herringbones. To further explore the template effect on the coordination of Fe−I4CA, we changed the substrate to Au(100), whose row-reconstruction pattern was different from that of Au(111).[31−33] The self-assembly of I4CA molecules on Au(100) at room temperature resulted in the formation of rectangular pores (Figure 5a). As the number of molecules on top of the reconstructed rows was larger than that between the reconstructed rows, the molecules in the STM images of the rectangular pores on Au(100) appeared brighter and darker. After depositing iron atoms on the sample, we observed that the molecules coordinated with the iron atoms, forming tetrameric clusters on top of and in between the reconstructed rows in Figure 5b,c. The template of Au(100) changed the distribution of tetrameric clusters. The Fe−I4CA coordination chains (Figure 5d) were formed upon increasing the annealing temperature to 350 K. The coordination chains with $[(Fe_2)(carboxylate)_3(pyrrolyl)_1]$ centers were the same as those on Au(111) in Figure 3b, except that the orientation of the coordination chains deviated from the direction of the reconstructed rows.

To elucidate the discrimination of the assemblies on Au(111) and Au(100), we studied the coordination of Fe−I4CA on Ag(111), a flat substrate without surface reconstruction. I4CA molecules on Ag(111) self-assembled into hexagonal pores at room temperature as shown in Figure 6a. The two carboxylic groups at the center of the molecular dimer in white boxes appeared darker than those in yellow boxes in the close-up STM image (Figure 6b). The carboxylic groups were dehydrogenated and hence appeared dark on the surface, which had been reported even in a previous study.[34] According to DFT calculations, the intermolecular forces of the dark dimers may be ionic hydrogen bonding[35] between the −COOH groups and $-COO^-$ groups. Three molecules interacted with each other by three ionic hydrogen bonds: O···H−O, N···H−O, and C···H−O, forming the basic unit of

https://dx.doi.org/10.1021/acs.jpcc.9b11599
J. Phys. Chem. C 2020, 124, 7790−7796

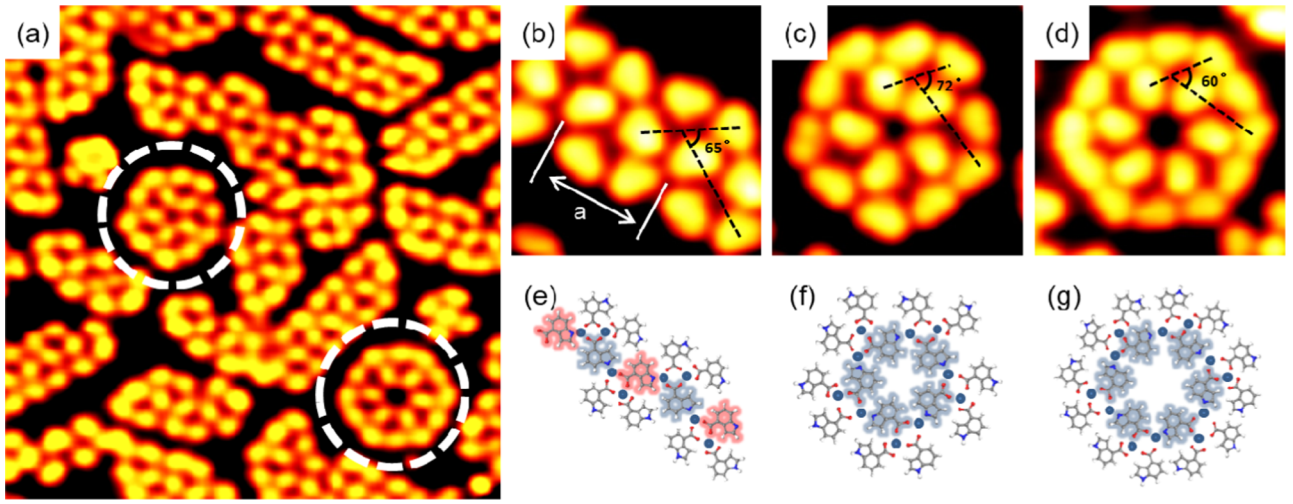

Figure 4. (a) STM topographs of the Fe−I4CA coordination structures obtained after being annealed at 400 K on Au(111). STM images (b−d) and corresponding molecular models (e−g) for tetramer chains and wheel-like structures having five and six hubs are displayed in order. The red and blue molecules in (e)−(g) represent the two adsorption chiralities that had an influence on the coordination structures. Imaging parameters: (a) V = 1 V, I = 50 pA, 26.6 × 26.6 nm^2; (b) V = 1 V, I = 20 pA, 5.8 × 5.8 nm^2; (c) V = 10 mV, I = 100 pA, 6.3 × 6.3 nm^2; and (d) V = 10 mV, I = 100 pA, 6.9 × 6.9 nm^2.

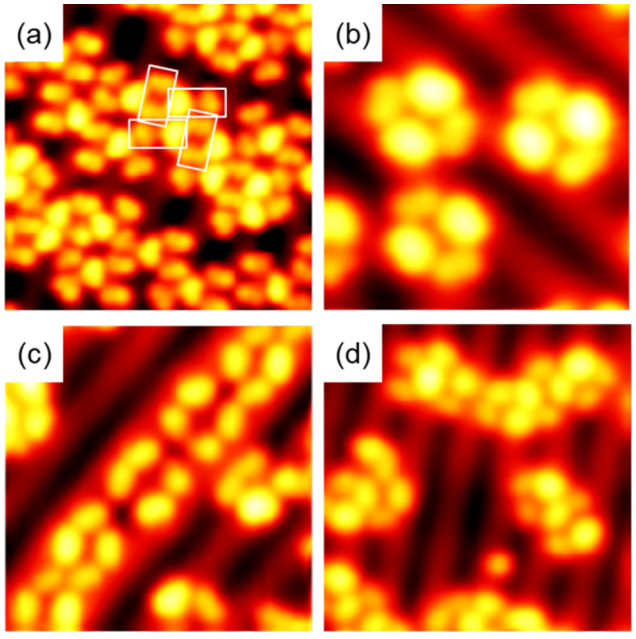

Figure 5. (a) STM image showing the self-assembly of I4CA on Au(100). The molecular dimers in white boxes formed rectangular pores. (b, c) STM images of Fe−I4CA coordination structures at room temperature. (b) Tetrameric clusters sitting on the reconstructed rows. (c) Tetrameric clusters located between the reconstructed rows. (d) STM images of Fe−I4CA coordination chains at 350 K. Imaging parameters: (a) V = 100 mV, I = 100 pA, 14.0 × 14.0 nm^2; (b) V = 10 mV, I = 50 pA, 8.4 × 8.4 nm^2; (c) V = 10 mV, I = 50 pA, 11.2 × 11.2 nm^2; and (d) V = 1 V, I = 20 pA, 14.0 × 14.0 nm^2.

such a structure. Figure 6c presents a molecular model of this assembly. Due to the high stability of the ionic hydrogen bonding structure, Fe atoms aggregated to form Fe clusters upon deposition onto the sample at room temperature. Hardly did we observe any I4CA molecules coordinating to Fe atoms. After annealing the sample at 350 K, Fe atoms and I4CA molecules formed a disordered coordination network, which could help to improve our understanding of the nature of the condensed disordered system.[36] The irregular network in the STM image (Figure 6d) consisted of pores of different sizes interconnected by two kinds of nodes. The high-resolution STM image (Figure 6e) revealed I4CA and Fe positioning within the coordination network. The predominant bifurcation motifs were the 4-fold $[(Fe_2)(carboxylate)_x(pyrrolyl)_{4-x}]$ (x = 2, 3) and the 3-fold $[(Fe)(carboxylate)_1(pyrrolyl)_2]$ nodes. The 4-fold $[(Fe_2)(carboxylate)_x(pyrrolyl)_{4-x}]$ (x = 2,3) node is similar to that in Figure 3f, and the 3-fold $[(Fe)(carboxylate)_1(pyrrolyl)_2]$ node model is shown in Figure 6f. A 2D ordered coordination network with $[(Fe_2)(carboxylate)_2(pyrrolyl)_2]$ centers was obtained by annealing the sample at a temperature of about 420 K (Figure 6g). Through coordination of the carboxyl and pyrrolyl groups with Fe, every molecule in the $[(Fe_2)(carboxylate)_4]$ tetramers was shared by four adjacent tetramers. The position of Fe atoms and I4CA molecules in the network is clearly demonstrated in Figure 6h, and the corresponding model is shown in Figure 6i. 2D coordination networks were observed on Ag(111) rather than on Au surfaces due to the reconstruction of the Au surface, which limited the growth of the coordination network.

CONCLUSIONS

Our investigation has demonstrated a stepwise coordination process of iron atoms and I4CA molecules on the Au(111) surface. Taking advantage of the differences in the potential barrier of the deprotonation process for the pyrrolyl and carboxyl groups, we successfully controlled the coordination path (iron atoms coordinated to the carboxyl and the pyrrolyl groups in sequence) by stepwise thermal annealing. The self-assembly of I4CA molecules on the Au(111) surface resulted in rectangular and hexagonal porous structures at room temperature. The carboxyl group reacted with Fe atoms to form tetramers at room temperature in a deprotonation process. Also, the deprotonation of pyrrolyl group occurred after annealing at higher temperatures to form coordinated tetramer chains and rotiform structures. The reconstruction on Au(100) altered the arrangement of tetrameric clusters and 1D

https://dx.doi.org/10.1021/acs.jpcc.9b11599
J. Phys. Chem. C 2020, 124, 7790−7796

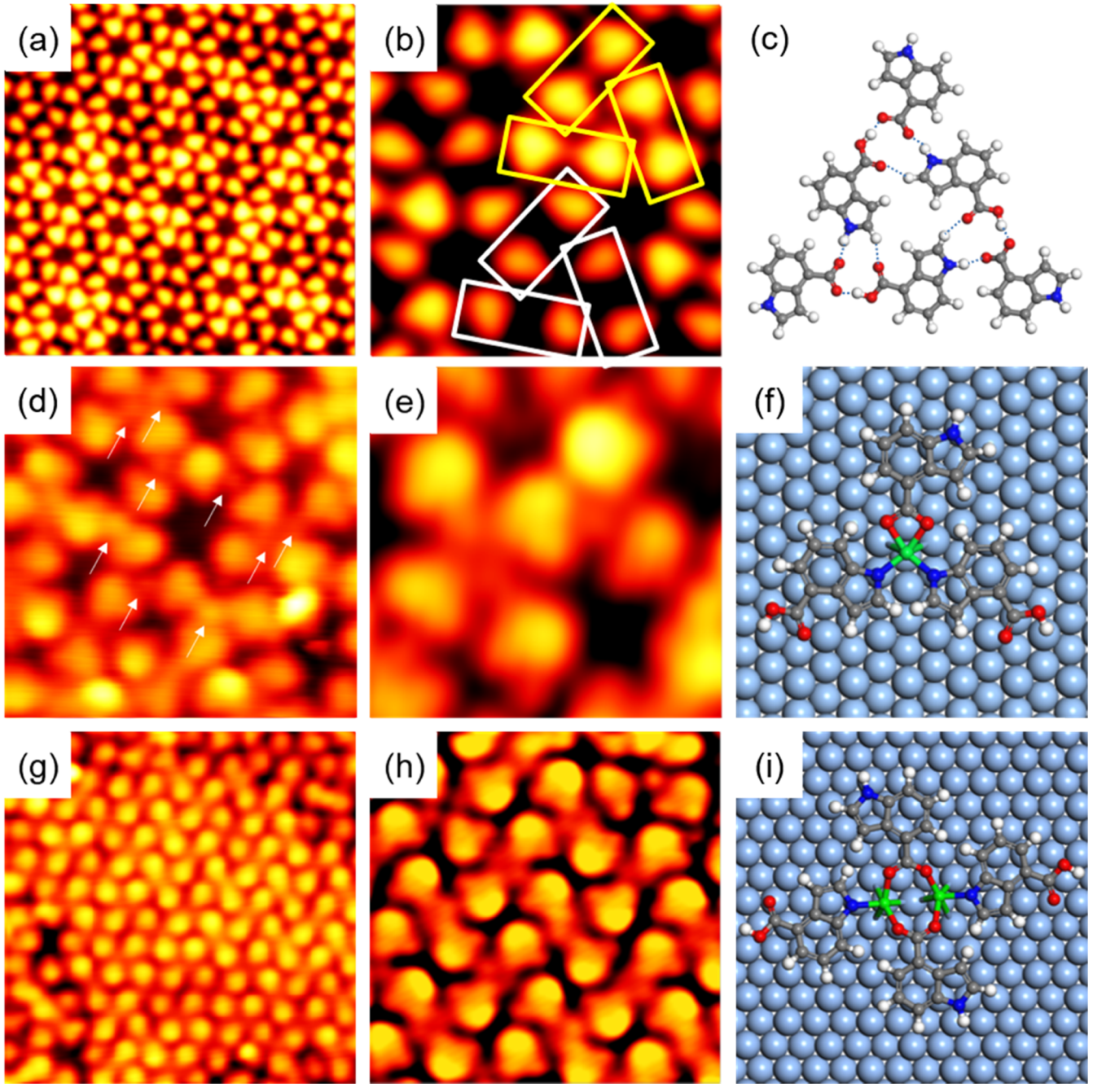

Figure 6. (a) STM images showing hexagonal pores formed by the self-assembly of I4CA on Ag(111). (b) High-resolution STM image of the hexagonal pores. The hydrogen bonding and ionic hydrogen bonding structures are highlighted by yellow and white boxes. (c) Tentative model of the ionic hydrogen bonding structures. (d, e) STM images of the Fe−I4CA coordination network formed at 350 K with the corresponding structural model in (f). (g, h) STM images of the Fe−I4CA coordinate 2D network at 420 K with the corresponding structural models in (i). All models were optimized using DFT calculations. Imaging parameters: (a) V = 10 mV, I = 50 pA, 18.8 × 18.8 nm^2; (b) V = 1 mV, I = 50 pA, 6.5 × 6.5 nm^2; (d) V = 1 mV, I = 50 pA, 9.8 × 9.8 nm^2; (e) V = 1 mV, I = 50 pA, 4.1 × 4.1 nm^2; (g) V = 1 mV, I = 50 pA, 14.0 × 14.0 nm^2; and (h) V = 1 mV, I = 800 pA, 6.7 × 6.7 nm^2.

coordination chains. 2D coordination networks could be obtained on Ag(111) without the influence of surface reconstructions.

AUTHOR INFORMATION

Corresponding Author

Yongfeng Wang − *Key Laboratory for the Physics and Chemistry of Nanodevices, Department of Electronics, Peking University, Beijing 100871, China; Beijing Academy of Quantum Information Sciences, Beijing 100193, China;* orcid.org/0000-0002-8171-3189; Email: yongfengwang@pku.edu.cn

Authors

Qiang Xue − *Key Laboratory for the Physics and Chemistry of Nanodevices, Department of Electronics, Peking University, Beijing 100871, China*

Na Xue − *Peking University Information Technology Institute (Tianjin Binhai), Tianjin 300450, China*

https://dx.doi.org/10.1021/acs.jpcc.9b11599
J. Phys. Chem. C 2020, 124, 7790−7796

Jie Li − *Peking University Information Technology Institute (Tianjin Binhai), Tianjin 300450, China*
Yaru Li − *Peking University Information Technology Institute (Tianjin Binhai), Tianjin 300450, China*
Ruoning Li − *Key Laboratory for the Physics and Chemistry of Nanodevices, Department of Electronics, Peking University, Beijing 100871, China*
Yajie Zhang − *Key Laboratory for the Physics and Chemistry of Nanodevices, Department of Electronics, Peking University, Beijing 100871, China;* orcid.org/0000-0001-7096-1040
Na Li − *Key Laboratory for the Physics and Chemistry of Nanodevices, Department of Electronics, Peking University, Beijing 100871, China;* orcid.org/0000-0001-6924-8387
Ziyong Shen − *Key Laboratory for the Physics and Chemistry of Nanodevices, Department of Electronics, Peking University, Beijing 100871, China*
Shimin Hou − *Key Laboratory for the Physics and Chemistry of Nanodevices, Department of Electronics, Peking University, Beijing 100871, China;* orcid.org/0000-0002-5042-4405

Complete contact information is available at: https://pubs.acs.org/10.1021/acs.jpcc.9b11599

Author Contributions

The manuscript was written through the contributions of all authors. All authors have given approval to the final version of the manuscript.

Notes

The authors declare no competing financial interest.

■ ACKNOWLEDGMENTS

This work was supported by the Ministry of Science and Technology (2018YFA0306003 and 2017YFA0205003) and the National Natural Science Foundation of China (21972002 and 21902003). DFT calculations were carried out on TianHe-1A at the National Supercomputer Center in Tianjin and supported by the High-Performance Computing Platform of Peking University.

■ REFERENCES

(1) Moulton, B.; Zaworotko, M. J. From molecules to crystal engineering: supramolecular isomerism and polymorphism in network solids. *Chem. Rev.* **2001**, *101*, 1629−1658.
(2) Yaghi, O. M.; O'Keeffe, M.; Ockwig, N. W.; Chae, H. K.; Eddaoudi, M.; Kim, J. Reticular synthesis and the design of new materials. *Nature* **2003**, *423*, 705−714.
(3) García-García, P.; Müller, M.; Corma, A. MOF catalysis in relation to their homogeneous counterparts and conventional solid catalysts. *Chem. Sci.* **2014**, *5*, 2979−3007.
(4) Ramaswamy, P.; Wong, N. E.; Shimizu, G. K. H. MOFs as proton conductors−challenges and opportunities. *Chem. Soc. Rev.* **2014**, *43*, 5913−5932.
(5) Tian, Y.; Cong, J.; Shen, S.; Chai, Y.; Yan, L.; Wang, S.; Sun, Y. Electric control of magnetism in a multiferroic metal−organic framework. *Phy. Status Solidi RRL* **2014**, *8*, 91−94.
(6) Lee, J. Y.; Li, J.; Jagiello, J. Gas sorption properties of microporous metal organic frameworks. *J. Solid State Chem.* **2005**, *178*, 2527−2532.
(7) Rabbani, M. G.; El-Kaderi, H. M. Template-free synthesis of a highly porous benzimidazole-linked polymer for CO_2 capture and H_2 storage. *Chem. Mater.* **2011**, *23*, 1650−1653.
(8) He, Y.; Zhang, Z.; Xiang, S.; Fronczek, F. R.; Krishna, R.; Chen, B. A microporous metal−organic framework for highly selective separation of acetylene, ethylene, and ethane from methane at room temperature. *Chem. - Eur. J.* **2012**, *18*, 613−619.
(9) Zheng, B.; Bai, J.; Duan, J.; Wojtas, L.; Zaworotko, M. J. Enhanced CO_2 binding affinity of a high-uptake rht-type metal−organic framework decorated with acylamide groups. *J. Am. Chem. Soc.* **2011**, *133*, 748−751.
(10) Dong, L.; Gao, Z. A.; Lin, N. Self-assembly of metal−organic coordination structures on surfaces. *Prog. Surf. Sci.* **2016**, *91*, 101−135.
(11) Langner, A.; Tait, S. L.; Lin, N.; Chandrasekar, R.; Meded, V.; Fink, K.; Ruben, M.; Kern, K. Selective Coordination Bonding in Metallo-Supramolecular Systems on Surfaces. *Angew. Chem., Int. Ed.* **2012**, *51*, 4327−4331.
(12) Stepanow, S.; Lingenfelder, M.; Dmitriev, A.; Spillmann, H.; Delvigne, E.; Lin, N.; Deng, X.; Cai, C.; Barth, J. V.; Kern, K. Steering molecular organization and host−guest interactions using two-dimensional nanoporous coordination systems. *Nat. Mater.* **2004**, *3*, 229−233.
(13) Lin, N.; Stepanow, S.; Vidal, F.; Barth, J. V.; Kern, K. Manipulating 2D metal−organic networks via ligand control. *Chem. Commun.* **2005**, 1681−1683.
(14) Shchyrba, A.; Wäckerlin, C.; Nowakowski, J.; Nowakowska, S.; Björk, J.; Fatayer, S.; Girovsky, J.; Nijs, T.; Martens, S. C.; Kleibert, A.; Stohr, M.; et al. Controlling the dimensionality of on-surface coordination polymers via endo-or exoligation. *J. Am. Chem. Soc.* **2014**, *136*, 9355−9363.
(15) Liu, J.; Lin, T.; Shi, Z.; Xia, F.; Dong, L.; Liu, P. N.; Lin, N. Structural transformation of two-dimensional metal−organic coordination networks driven by intrinsic in-plane compression. *J. Am. Chem. Soc.* **2011**, *133*, 18760−18766.
(16) Li, Y.; Xiao, J.; Shubina, T. E.; Chen, M.; Shi, Z.; Schmid, M.; Steinruck, H.-P.; Gottfried, J. M.; Lin, N. Coordination and metalation bifunctionality of Cu with 5, 10, 15, 20-tetra (4-pyridyl) porphyrin: toward a mixed-valence two-dimensional coordination network. *J. Am. Chem. Soc.* **2012**, *134*, 6401−6408.
(17) Lyu, G.; Zhang, R.; Zhang, X.; Liu, P. N.; Lin, N. On-surface assembly of low-dimensional Pb-coordinated metal−organic structures. *J. Mater. Chem. C* **2015**, *3*, 3252−3257.
(18) Yan, L.; Kuang, G.; Zhang, Q.; Shang, X.; Liu, P. N.; Lin, N. Self-assembly of a binodal metal−organic framework exhibiting a demi-regular lattice. *Faraday Discuss.* **2017**, *204*, 111−121.
(19) Lin, T.; Shang, X. S.; Adisoejoso, J.; Liu, P. N.; Lin, N. Steering on-surface polymerization with metal-directed template. *J. Am. Chem. Soc.* **2013**, *135*, 3576−3582.
(20) Li, C.; Zhang, X.; Li, N.; Wang, Y.; Yang, J.; Gu, G.; Zhang, Y.; Hou, S.; Peng, L.; Wu, K.; et al. Construction of Sierpinski Triangles up to the Fifth Order. *J. Am. Chem. Soc.* **2017**, *139*, 13749−13753.
(21) Jansen, R. J. J.; Van Bekkum, H. XPS of nitrogen-containing functional groups on activated carbon. *Carbon* **1995**, *33*, 1021−1027.
(22) Adisoejoso, J.; Li, Y.; Liu, J.; Liu, P. N.; Lin, N. Two-dimensional metallo-supramolecular polymerization: toward size-controlled multi-strand polymers. *J. Am. Chem. Soc.* **2012**, *134*, 18526−18529.
(23) Buchner, F.; Flechtner, K.; Bai, Y.; Zillner, E.; Kellner, I.; Steinrück, H.-P.; Marbach, H.; Gottfried, M. Coordination of iron atoms by tetraphenylporphyrin monolayers and multilayers on Ag (111) and formation of iron-tetraphenylporphyrin. *J. Phys. Chem. C* **2008**, *112*, 15458−15465.
(24) Urgel, J. I.; Ecija, D.; Lyu, G.; Zhang, R.; Palma, C.-A.; Auwärter, W.; Lin, N.; Barth, J. V. Quasicrystallinity expressed in two-dimensional coordination networks. *Nat. Chem.* **2016**, *8*, 657.
(25) Horcas, I.; Fernández, R.; Gómez-Rodríguez, J. M.; Colchero, J.; Gómez-Herrero, J.; Baro, A. M. WSXM: A software for scanning probe microscopy and a tool for nanotechnology. *Rev. Sci. Instrum.* **2007**, *78*, No. 013705.
(26) De Marchi, F.; Cui, D.; Lipton-Duffin, J.; Santato, C.; Macleod, J. M.; Rosei, F. Self-assembly of indole-2-carboxylic acid at graphite and gold surfaces. *J. Chem. Phys.* **2015**, *142*, No. 101923.
(27) Seitsonen, A. P.; Lingenfelder, M.; Spillmann, H.; Dmitriev, A.; Stepanow, S.; Lin, N.; Kern, K.; Barth, J. V. Density Functional Theory Analysis of Carboxylate-Bridged Diiron Units in Two-

Dimensional Metal−Organic Grids. *J. Am. Chem. Soc.* **2006**, *128*, 5634−5635.
(28) Langner, A.; Tait, S. L.; Lin, N.; Rajadurai, C.; Ruben, M.; Kern, K. Self recognition and self selection in multicomponent supramolecular coordination networks on surfaces. *Proc. Natl. Acad. Sci. U.S.A.* **2007**, *104*, 17927−17930.
(29) Wang, Y.; Ge, X.; Manzano, C.; Kröger, J.; Berndt, R.; Hofer, W. A.; Tang, H.; Cerda, J. Supramolecular patterns controlled by electron interference and direct intermolecular interactions. *J. Am. Chem. Soc.* **2009**, *131*, 10400−10402.
(30) Böhringer, M.; Morgenstern, K.; Schneider, W.-D.; Wühn, M.; Wöll, C.; Berndt, R. Self-assembly of 1-nitronaphthalene on Au (111). *Surf. Sci.* **2000**, *444*, 199−210.
(31) Havu, P.; Blum, V.; Havu, V.; Rinke, P.; Scheffler, M. Large-scale surface reconstruction energetics of Pt (100) and Au (100) by all-electron density functional theory. *Phys. Rev. B* **2010**, *82*, No. 161418.
(32) Bengió, S.; Navarro, V.; González-Barrio, M. A.; Cortés, R.; Vobornik, I.; Michel, E. G.; Mascaraque, A. Electronic structure of reconstructed Au (100): Two-dimensional and one-dimensional surface states. *Phys. Rev. B* **2012**, *86*, No. 045426.
(33) Alemani, M.; Selvanathan, S.; Ample, F.; Peters, M. V.; Rieder, K.-H.; Moresco, F.; Joachim, C.; Hecht, S.; Grill, L. Adsorption and switching properties of azobenzene derivatives on different noble metal surfaces: Au (111), Cu (111), and Au (100). *J. Phys. Chem. C* **2008**, *112*, 10509−10514.
(34) Schmitt, T.; Hammer, L.; Schneider, M. A. Evidence for On-Site Carboxylation in the Self-Assembly of 4, 4′-Biphenyl Dicarboxylic Acid on Cu (111). *J. Phys. Chem. C* **2016**, *120*, 1043−1048.
(35) Payer, D.; Comisso, A.; Dmitriev, A.; Strunskus, T.; Lin, N.; Wöll, C.; DeVita, A.; Barth, J. V.; Kern, K. Ionic Hydrogen Bonds Controlling Two-Dimensional Supramolecular Systems at a Metal Surface. *Chem. - Eur. J.* **2007**, *13*, 3900−3906.
(36) Marschall, M.; Reichert, J.; Weber-Bargioni, A.; Seufert, K.; Auwärter, W.; Klyatskaya, S.; Zoppellaro, G.; Ruben, M.; Barth, J. V. Random two-dimensional string networks based on divergent coordination assembly. *Nat. Chem.* **2010**, *2*, 131−137.

https://dx.doi.org/10.1021/acs.jpcc.9b11599
J. Phys. Chem. C 2020, 124, 7790−7796